Preprints.org

Article

Not peer-reviewed version

Integrated Network Pharmacology and Metabolomics to Reveal the Mechanisms of the Combined Intervention of Ligustrazine and Sinomenine in CCI-Induced Neuropathic Pain Rats

Tao Li *, Zhiguo Wang *, Zhaoyue Yuan, Xiaoliang Zhao, Yan Zhang, Yue Jiao, Yang Liu, Chang Gao, Jidan Zhang, Yanyan Ma

Posted Date: 23 January 2025

doi: 10.20944/preprints202501.1776.v1

Keywords: Neuropathic pain; Ligustrazine; Sinomenine; Tyrosine metabolism; Phenylalanine metabolism

Preprints.org is a free multidisciplinary platform providing preprint service that is dedicated to making early versions of research outputs permanently available and citable. Preprints posted at Preprints.org appear in Web of Science, Crossref, Google Scholar, Scilit, Europe PMC.

Copyright: This open access article is published under a Creative Commons CC BY 4.0 license, which permit the free download, distribution, and reuse, provided that the author and preprint are cited in any reuse.

Preprints.org (www.preprints.org) | NOT PEER-REVIEWED | Posted: 23 January 2025 doi:10.20944/preprints202501.1776.v1

Disclaimer/Publisher's Note: The statements, opinions, and data contained in all publications are solely those of the individual author(s) and contributor(s) and not of MDPI and/or the editor(s). MDPI and/or the editor(s) disclaim responsibility for any injury to people or property resulting from any ideas, methods, instructions, or products referred to in the content.

Article

Integrated Network Pharmacology and Metabolomics to Reveal the Mechanisms of the Combined Intervention of Ligustrazine and Sinomenine in CCI-Induced Neuropathic Pain Rats

Zhaoyue Yuan [1,†], Xiaoliang Zhao [1,†], Yan Zhang [2,†], Yue Jiao [1], Yang Liu [1], Chang Gao [1], Jidan Zhang [1], Yanyan Ma [1], Zhiguo Wang [1,*] and Tao Li [1,2,*]

[1] Experimental Research Center, China Academy of Chinese Medical Sciences, Beijing 100700, China; zyueyuan1118@163.com; zhaoxiaoliang1218@aliyun.com; 1784865127@qq.com; jiaoyue_medicine@163.com; echoinapril@163.com; gaochangmail2022@163.com; zjdjy620@163.com; yanyan8098@126.com

[2] Institute of Chinese Materia Medica, China Academy of Chinese Medical Sciences, Beijing 100700

* Correspondence: hndxlitao@163.com (Tao Li), zhgw68_8@tom.com (Zhiguo Wang)

† These authors contributed equally to this work.

Abstract: Neuropathic pain (NP) is a chronic pain resulting from injury or dysfunction of the nerves or spinal cord. Previous studies have shown that the combination of ligustrazine (LGZ) and sinomenine (SIN) exerts a synergistic antinociceptive effect in peripheral and central NP models. This study aims to evaluate the pharmacodynamic characteristics of LGZ and SIN in a chronic constriction injury (CCI)-induced NP models in rats, and to analyze its molecular regulatory mechanisms from the perspectives of network pharmacology and metabolomics. Firstly, a comprehensive analgesic evaluation including the mechanical withdrawal threshold test, cold allodynia test, and the incapacitance test was performed after 1, 2 and 3 days of intervention. The sciatic nerve histopathological changes were observed, and inflammatory factor analysis were conducted. Secondly, the pain-related targets of LGZ and SIN were systematically analyzed based on network pharmacology. The differential metabolites in the plasma and cerebrospinal fluid (CSF) were screened, and their content were quantified using LC-MS metabolomics technology. Finally, the key metabolic pathways with crucial role of LGZ and SIN in treating NP was identified from a joint analysis of the potential targets and the differential metabolites. The combination of LGZ and SIN significantly alleviated pain-like behaviors of CCI rats time- and dose-dependently, and the therapeutic effect was notably superior to that of LGZ or SIN alone. The combination of LGZ and SIN could improve pathological damage to the sciatic nerve and regulate the levels of inflammatory cytokine. Network pharmacology analysis revealed that LGZ and SIN have 6 shared pain-related targets, while LGZ have 16 distinct pain-related targets and SIN have 52 distinct pain-related targets. The metabolomics analyses revealed that 54 differential metabolites in plasma and 17 differential metabolites in CSF were associated with the combined intervention of LGZ and SIN. Finally, through integrated analysis of the core targets and differential metabolites, tyrosine metabolism, phenylalanine metabolism, and arginine and proline metabolism were identified as potential key metabolic pathways underlying the therapeutic effects of LGZ and SIN in CCI treatment. This study provides an integrated approach to elucidate the molecular mechanisms underlying the combined use of LGZ and SIN in the treatment of NP. Furthermore, the findings offer new experimental evidence to support the clinical application of LGZ and SIN in the treatment of NP.

Keywords: Neuropathic pain; Ligustrazine; Sinomenine; Tyrosine metabolism; Phenylalanine metabolism

© 2025 by the author(s). Distributed under a Creative Commons CC BY license.

Preprints.org (www.preprints.org) | NOT PEER-REVIEWED | Posted: 23 January 2025 doi:10.20944/preprints202501.1776.v1

1. Introduction

Neuropathic pain (NP) is a chronic pain characterized by persistent or intermittent spontaneous pain, often accompanied by evoked pain, particularly cold or mechanical allodynia. NP arises from injury or malfunction of the nerves or spinal cord and is commonly prevalent in clinical practice. It may emerge as a secondary condition from a variety of clinical disorders, including trauma, stroke, infection, diabetes, multiple sclerosis, and cancer[1,2]. Globally, the incidence of NP accounts for 6.9% to 10% of the total population [3]. NP leads to significant reductions in both quality of life and behavioral function, placing a heavy physical and psychological burden on patients[4]. The pathophysiology of NP is complex and multifactorial. Despite the availability of various interventions based on different mechanisms, the results of NP treatment are still unsatisfactory[5]. Commonly used medications for NP, such as nonsteroidal anti-inflammatory drugs and opioids, often cause adverse effects, including dizziness, drowsiness, arrhythmias, and issues related to tolerance when used alone[6]. Consequently, the development of combination therapies targeting multiple analgesic mechanisms has become a promising insight in the treatment of NP. Indeed, clinical approaches to chronic pain often evolve from initial monotherapy to combination therapy as a more effective means of addressing the complex nature of NP[7].

Traditional Chinese medicine (TCM) boasts an extensive history in the treatment of NP, with many Chinese herbal medicines and their active compounds reported to alleviate NP symptoms[8]. These therapies represent a rich source for the screening of potential combination drugs for NP treatment. Chuanxiong Rhizoma, derived from the rhizome of *Ligusticum chuanxiong* Hort., has been widely used in traditional medicine since the Han Dynasty (~1800 years ago), though it is typically employed as an adjunctive or supporting medicine according to TCM theory. Ligustrazine (LGZ), the major active ingredient of Chuanxiong Rhizoma, exhibits outstanding pharmacological effects in blood circulation or peripheral improving microcirculation. Its formulations, such as ligustrazine injection and salvia miltiorrhiza-ligustrazine injection are primarily used in China for the treatment of occlusive cerebrovascular diseases[9,10]. As reported, LGZ exhibited therapeutic effects in various pain animal models, such as migraine[11] and spinal cord injury-induced NP [12]. Sinomenii Caulis, sourced from the stems of *Sinomenium acutum* (Thunb.) Rehd. et Wils. and *Sinomenium acutum* var. *cinereum* Rehd. et Wils. Sinomenine (SIN), the active compound in Sinomenii Caulis, is used clinically for the treatment of rheumatism, rheumatoid arthritis, and related pain symptoms[13,14]. SIN has demonstrated analgesic effects on inflammatory pain[15], spared nerve injury-induced NP[16], and diabetic peripheral NP[17], exerting both anti-inflammatory and analgesic mechanisms. Our previous studies have shown that the combination of LGZ and SIN was effective in alleviating pain in various NP models, including those induced by sciatic nerve injury, trigeminal nerve injury, and spinal cord injury[18]. Moreover, the combination of LGZ and SIN exhibited a synergistic analgesic effect, allowing for a reduction in the individual dosages of each compound. Both LGZ and SIN have been reported to have numerous potential targets and pathways, but the specific mechanisms underlying their analgesic effected in NP remain unclear.

Network pharmacology analyzes the relationships among drugs, targets, and diseases through network-based approaches, making it particularly well-suited for elucidating core targets and pathways in treating complex diseases by TCM, which characterized by "multi-target" and "multi-pathway"[19]. By offering a systems-level perspective, network pharmacology uncovers the potential molecular mechanisms of TCM, shedding light on its holistic therapeutic effects[20,21]. Metabolomics, an essential component of systems biology, utilizes high-throughput and highly sensitive instruments to conduct comprehensive profiling of endogenous components within biological samples. By integrating multivariate statistical methods, metabolomics can reveal changes in endogenous metabolites under vatious physiological, pathological, or toxicological conditions[22], enabling the identification of the key metabolic pathways within the organism[23]. Therefore, the integration of metabolomics with network pharmacology can provide a more comprehensive understanding of the metabolic pathways and network regulatory mechanisms of the combined therapy in treating complex disease.

In this study, network pharmacology was initially used to predict the potential targets of LGZ and SIN in treating pain-related diseases, analyzing both their shared and distinct targets.

Preprints.org (www.preprints.org) | NOT PEER-REVIEWED | Posted: 23 January 2025 doi:10.20944/preprints202501.1776.v1

Subsequently, the analgesic effects of LGZ, SIN and their combination at different time points and dosages were comprehensively evaluated in a chronic constriction injury (CCI)-induced NP model in rats. Furthermore, the key metabolites in the plasma and cerebrospinal fluid (CSF) were screened, and their content were quantified using LC-MS metabolomics technology. Finally, a joint analysis of the potential targets and key metabolites was conducted to identify the crucial metabolic pathways through which LGZ and SIN exert their therapeutic effects in NP. The aim of this study was to elucidate the molecular mechanisms underlying the combined use of LGZ and SIN in treating NP. Additionally, this research aimed to offer new experimental evidence to support the clinical combined application of LGZ and SIN in treating NP.

2. Results

2.1. The Combination of LGZ and SIN Pharmacological Effects on CCI Rats

2.1.1. General Animal Condition

Following CCI surgery and treatment, all groups of rats exhibited an upward trend in body weight (Figure 1A). After administration, the Model group showed a slower rate of weight gain compared to the Sham group. Conversely, all treated groups exhibited greater body weight gain compared to the Model group, with the LGZ+SIN high-dose group showing the most significant weight increase. These findings suggested that the combined treatment of LGZ and SIN, positively affected the overall health status of CCI rats. Throughout the experiment, no significant toxic side effects were observed in any of the groups.

Preprints.org (www.preprints.org) | NOT PEER-REVIEWED | Posted: 23 January 2025 doi:10.20944/preprints202501.1776.v1

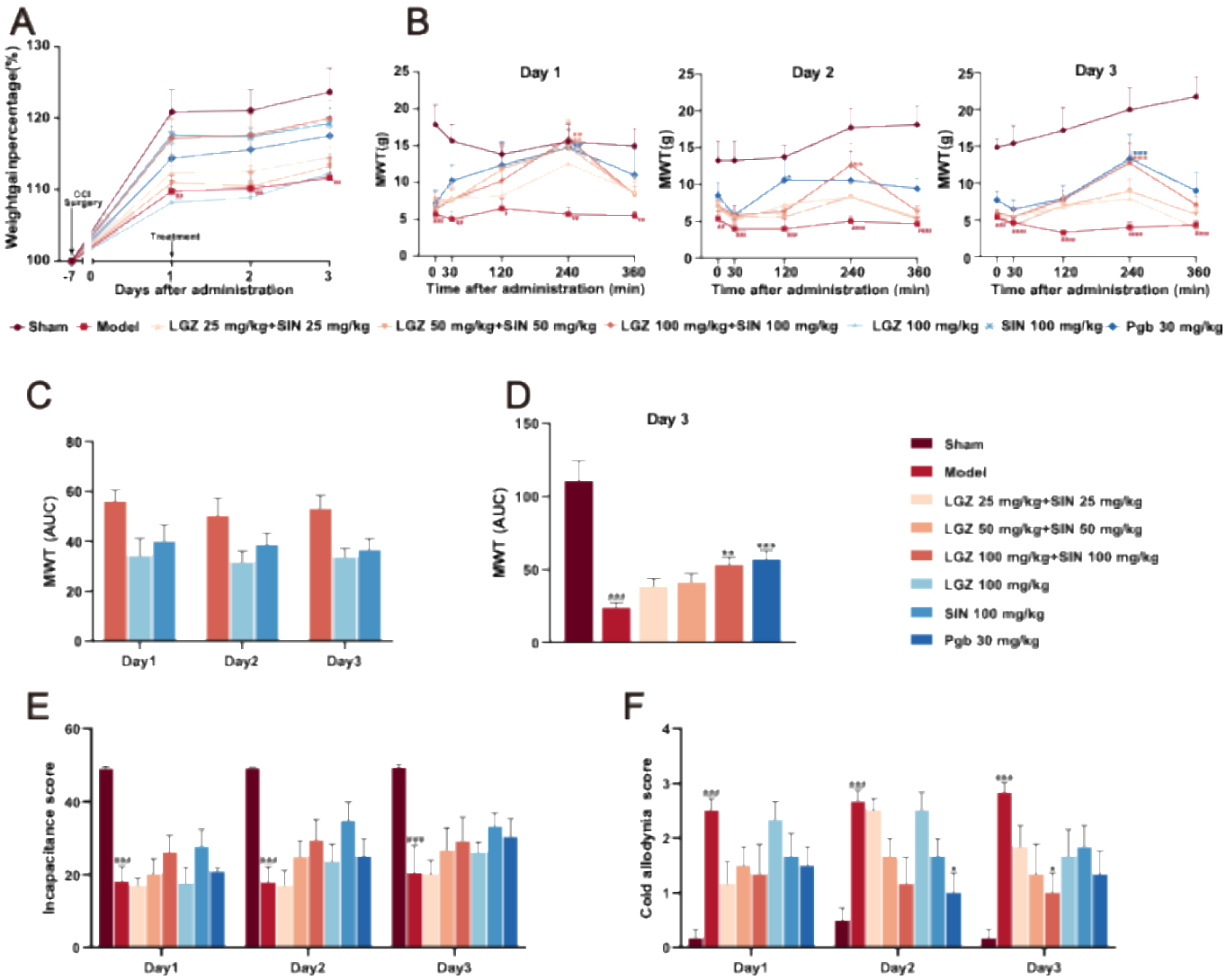

Figure 1. Analgesic effect of LGZ+SIN in CCI rats. (A)Body weight gain percentage. (B) MWT value after administration during 3 days of treatment. (C) AUC of MWT value on the third day of treatment. (D). AUC of MWT value per day during 3 days of treatment. (E) Cold allodynia score during 3 days of treatment. (F) Incapacitance score during 3 days of treatment. $^{\#}p < 0.05$, $^{\#\#}p < 0.01$, $^{\#\#\#}p < 0.001$ (compared to the Sham group). $^{*}p < 0.05$, $^{**}p < 0.01$, $^{***}p < 0.001$ (compared to the Model group).

2.1.2. The Combination of LGZ and SIN Improve Pain-Related Behaviors in CCI Rats

The MWT results indicated that, as early as 0.5 hours post-administration, the LGZ+SIN, LGZ, and SIN groups significantly increased the MWT, with the peak effect observed at 4 hours, demonstrating statistically significant differences. The pain-relieving trend was consistent across all treatment groups on days 1, 2, and 3 post-treatments. (Figure 1B). To further quantify the effects, the area under the curve (AUC) of MWT values measured at 0, 0.5, 2, 4, and 6 hours post-treatment was calculated. The MWT values measured on the 1st, 2nd and 3rd day after administration were used to calculate the AUC for the LGZ+SIN high-dose, LGZ, and SIN groups. The results showed that the AUC for MWT in the LGZ+SIN groups was consistently superior to that of either the LGZ or the SIN group alone on all days of administration (Figure 1C). Furthermore, the LGZ+SIN high-dose group could increase the AUC for MWT more than LGZ+SIN medium or low-dose group on the third day of treatment (Figure 1D). These results suggest that the combined use of LGZ and SIN effectively alleviated mechanical pain in CCI rats, with a superior effect compared to the individual use of LGZ or SIN.

Preprints.org (www.preprints.org) | NOT PEER-REVIEWED | Posted: 23 January 2025 doi:10.20944/preprints202501.1776.v1

The cold allodynia test results (Figure 1E) revealed that during the administration period, the cold pain scores of the model group were significantly higher than those of the sham group ($p < 0.001$), indicating hypersensitivity to cold pain in CCI rats. Over the 3-day treatment period, the cold pain sensitivity scores in the LGZ+SIN and the SIN groups showed a decreasing trend compared to the model group. On the third day of administration, the cold pain score in the LGZ+SIN high-dose group was significantly reduced ($p < 0.05$). These results suggested that the combined use of LGZ and SIN had a significant effect in alleviating cold pain sensitivity in CCI rats. As shown in Supplementary Figure S1, the cold allodynia score in LGZ+SIN groups decreased significantly at 4 hours after administration, especially in LGZ+SIN high-dose group. The result indicated that the combination of LGZ and SIN had best effect after 4 hours of administration.

The results of the incapacitance test (Figure 1F) showed that, compared to the sham group, the model group had a significantly reduced incapacitance score ($p < 0.01$), indicating the presence of spontaneous pain in the CCI rats. Compared to the model group, the incapacitance score in the LGZ+SIN, LGZ, and SIN groups showed an increasing trend following treatment, with more noticeable improvements on the 2nd and 3rd days of administration. These results suggested that the combined use of LGZ and SIN might alleviate spontaneous pain in CCI rats.

2.1.3. The Combination of LGZ and SIN Alleviate the Pathological Structure of the Sciatic Nerve

H&E staining of the sciatic nerve revealed that the sciatic nerve fibers in the Sham group rats had a regular and evenly distributed structure, with tightly arranged intact myelin sheaths. In contrast, the Model group rats showed loose and sparse arrangement of sciatic nerve fibers, with deformed myelin sheaths and significant infiltration of inflammatory cells. The sciatic nerve structure in the LGZ group was closer to normal, with more orderly arrangement. Although demyelination was present, it was less severe than that in the Model group, indicating a certain level degree of pathological recovery. Both the LGZ+SIN and SIN groups exhibited varying degrees of disorganized nerve fiber arrangement, demyelination, and inflammatory cell infiltration, but the extent of these changes was milder than in the Model group (Fig. 2 A). These results suggested that the combined use of LGZ and SIN, LGZ, and SIN had a beneficial effect on the pathological repair of the sciatic nerve in CCI rats.

2.1.4. The Combination of LGZ+SIN Attenuate Sciatic Nerve Inflammatory Levels in CCI Rats

The concentrations of IL-1β, IL-6, and TNF-α in the sciatic nerve of each group (Figure 2B) showed that, compared to the Sham group, the Model group had significantly lower levels of IL-1β, IL-6, and TNF-α. After three days of treatment, the SIN group exhibited a significant increase in IL-1β levels in the sciatic nerve compared to the Model group ($p < 0.01$), while both the LGZ+SIN and SIN groups showed a significant increase in TNF-α levels ($p < 0.05$). These results suggest that the combined use of LGZ and SIN, LGZ, and SIN had a beneficial effect in alleviating sciatic nerve inflammation in CCI rats.

Preprints.org (www.preprints.org) | NOT PEER-REVIEWED | Posted: 23 January 2025 doi:10.20944/preprints202501.1776.v1

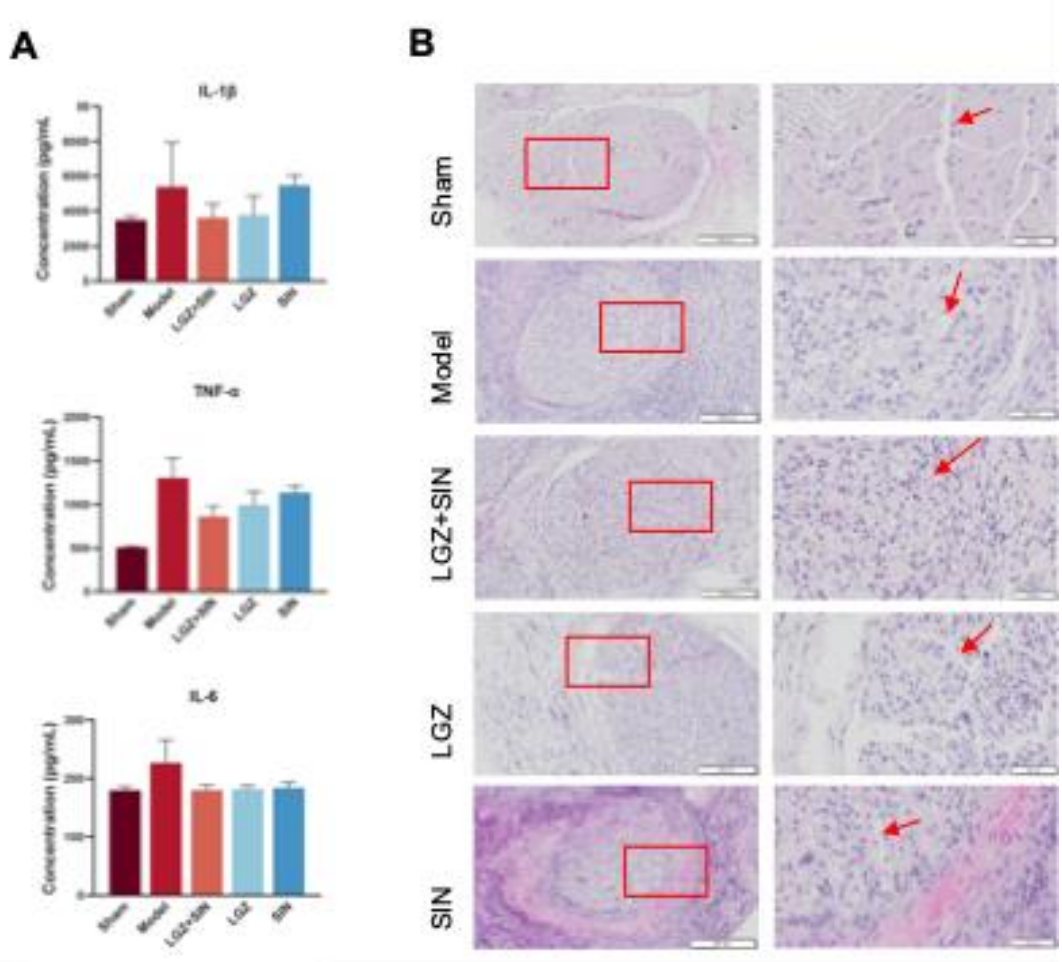

Figure 2. LGZ+SIN attenuated CCI induced sciatic nerve injury. (A) Inflammatory factor changes in sciatic nerve. (B) Representative images of HE staining of sciatic nerve. #$p < 0.05$, ##$p < 0.01$, ###$p < 0.001$ (compared to the Sham group). * $p < 0.05$, ** $p < 0.01$ (compared to the Model group).

2.2. Network Pharmacology Analysis

2.2.1. Potential Targets of LGZ and SIN in Pain Treatment

Through compound target database search and screening, 29 targets were identified for LGZ, and 100 targets were identified for SIN. The Genecards database revealed a total of 12,990 pain-related targets, with relevance scores ranging from a maximum of 100.27 to a minimum of 0.08. By screening targets with scores above the median, 3,303 pain-related targets were obtained. After merging the results from multiple databases and removing duplicates, a final set of 3,303 disease-related targets was identified.

The target information of the compounds was intersected with disease-related target genes on the GeneCards, and a Venn diagram was constructed (Figure 3A). Through this intersection, 22 pain-related targets were identified for LGZ, 58 pain-related targets for SIN, and 8 common targets between the two compounds. Among these, 16 specific targets were identified for LGZ, and 52 unique targets for SIN. These intersected genes were then input into the STRING 11.0 platform to construct the interaction networks based on protein-protein interactions (Figure 3B).

From this analysis, it was found that LGZ and SIN exerted their analgesic effects through six key targets: CA2, MPO, HTR6, MAOA, GSK3B, and BDKRB2. Additionally, both compounds also exhibited analgesic effects through their respective specific targets.

Preprints.org (www.preprints.org) | NOT PEER-REVIEWED | Posted: 23 January 2025 doi:10.20944/preprints202501.1776.v1

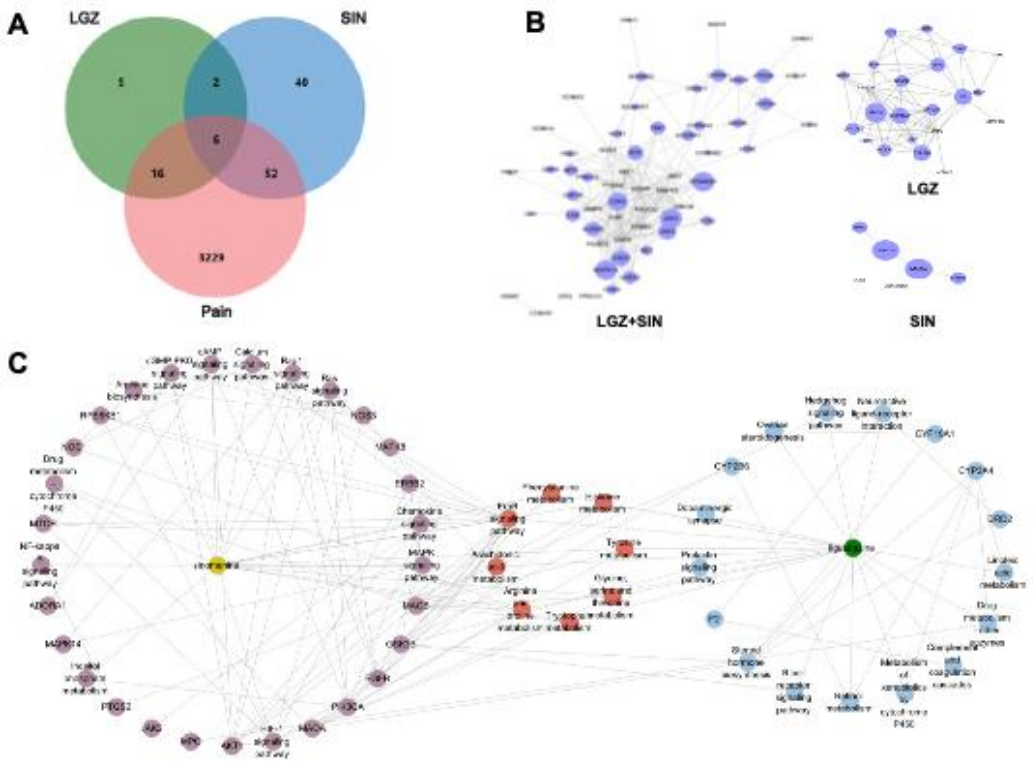

Figure 3. Exploring the effects of LGZ and SIN in pain based on network pharmacology. (A) Venn diagram. (B) Protein-protein network diagram. (C) Target-Pathway networks of LGZ and SIN through KEGG enrichment analysis of the targets.

2.2.2. Pain-relieving Pathways and Biological Function Differences Between LGZ and SIN

LGZ and SIN exhibited certain differences in their pain-relieving pathways and biological functions. The core targets of both compounds were analyzed using the Metascape, and KEGG and GO functional enrichment analyses were performed ($p < 0.01$). The top 30 GO terms were selected for the bar chart, and the top 20 KEGG pathways were visualized in a bubble chart (Supplementary Figure S2 A-B).

According to the KEGG analysis, LGZ primarily targets were related to the nervous system (Dopaminergic), signaling pathways (Synapse Neuroactive Ligand-Receptor Interaction, Hedgehog Signaling Pathway, ErbB Signaling Pathway), the immune system (B Cell Receptor Signaling Pathway), and the endocrine system (Prolactin Signaling Pathway). It also intervened the amino acid metabolism pathways such as tyrosine metabolism and tryptophan metabolism to exert its analgesic effect. Additionally, SIN exerted its analgesic effects by modulating signaling pathways (PI3K-Akt Signaling Pathway, TNF Signaling Pathway, Sphingolipid Signaling Pathway, ErbB Signaling Pathway), the nervous system (Dopaminergic), the immune system (IL-17 Signaling Pathway, T Cell Receptor Signaling Pathway), and the endocrine system (Prolactin Signaling Pathway, Insulin Signaling Pathway, Growth Hormone Synthesis, Secretion, and Action).

Through Venn diagram analysis, it was found that LGZ and SIN shared 6 common analgesic targets. By integrating these targets with the KEGG analysis, their intersecting genes primarily exerted analgesic effects by influencing the nervous system (Serotonergic Synapse, Dopaminergic Synapse), signaling pathways (Calcium Signaling Pathway, Neuroactive Ligand-Receptor Interaction, Hedgehog Signaling Pathway), and the endocrine system (Prolactin Signaling Pathway). These pathways, together with energy metabolism and amino acid metabolism pathways, were key to their analgesic effects.

To further clarify the combination pathways of LGZ and SIN for treating NP, all targets of them were mapped onto KEGG pathways to identify the pathways with $p < 0.05$. And the pathways were

Preprints.org (www.preprints.org) | NOT PEER-REVIEWED | Posted: 23 January 2025 doi:10.20944/preprints202501.1776.v1

selected and resulted in a target-pathway network (Figure 3C**)**. The results showed that LGZ and SIN shared 8 signaling pathways. These results proved that the treatment of the combination of LGZ and SIN for NP was a combination effects form.

In summary, LGZ and SIN shared 6 common pain-relieving target genes: CA2, HTR6, MAOA, GSK3B, BDKRB2, and MPO. Through an analysis of core targets, it was found that both compounds primarily affect the nervous system, immune system, and signaling pathways to exert their analgesic effects. However, a closer examination of the intersecting genes reveals that HTR6 and BDKRB2 are highly expressed in signaling pathways, while CA2 shows strong expression in the neuroactive ligand-receptor interaction pathway. Furthermore, the biological processes of these common genes suggested that they mainly influenced neurotransmitter breakdown and ion transport processes. This indicated that the combined use of LGZ and SIN might, to some extent, enhance the neuroprotective and signaling function of the system.

2.3. Metabolomic Analysis

A widely targeted metabolomics approach was employed to investigate the therapeutic mechanism of the combined use of LGZ and SIN, as well as their individual applications on CCI rats. To gain more detailed insights, plasma and CSF samples were analyzed separately in both positive and negative ion modes. The results from the positive and negative ion detection were subsequently merged and further analyzed to explore the underlying therapeutic mechanisms of treatment.

2.3.1. Differential Metabolites Analysis

PCA was performed on the data from each group. The PCA score plot revealed that the QC samples exhibited excellent stability, indicating that the analytical system was strong reliability, and the experimental data were of high quality and reliability. This suggested that the data met the criteria for metabolomics analysis. The details could be found in Supplementary Figure S3.

OPLS-DA was used to further identify potential biomarkers between the groups in plasma and CSF samples, respectively (Figure 4A-B). The OPLS-DA score plots clearly distinguished between the groups, indicating significant differences in metabolic profiles, and suggested that endogenous metabolites underwent noticeable changes among the groups.

To assess the robustness and validity of the OPLS-DA models, a random permutation test (n = 200) was performed (Supplementary Figure S4). The results indicated that none of the models were overfitted, confirming that the modeling outcomes were reliable. A model is considered valid when both the R^2Y and Q^2 values are greater than 0.5, which demonstrates that the model has good predictive power, and that the data are reliable.

Preprints.org (www.preprints.org) | NOT PEER-REVIEWED | Posted: 23 January 2025 doi:10.20944/preprints202501.1776.v1

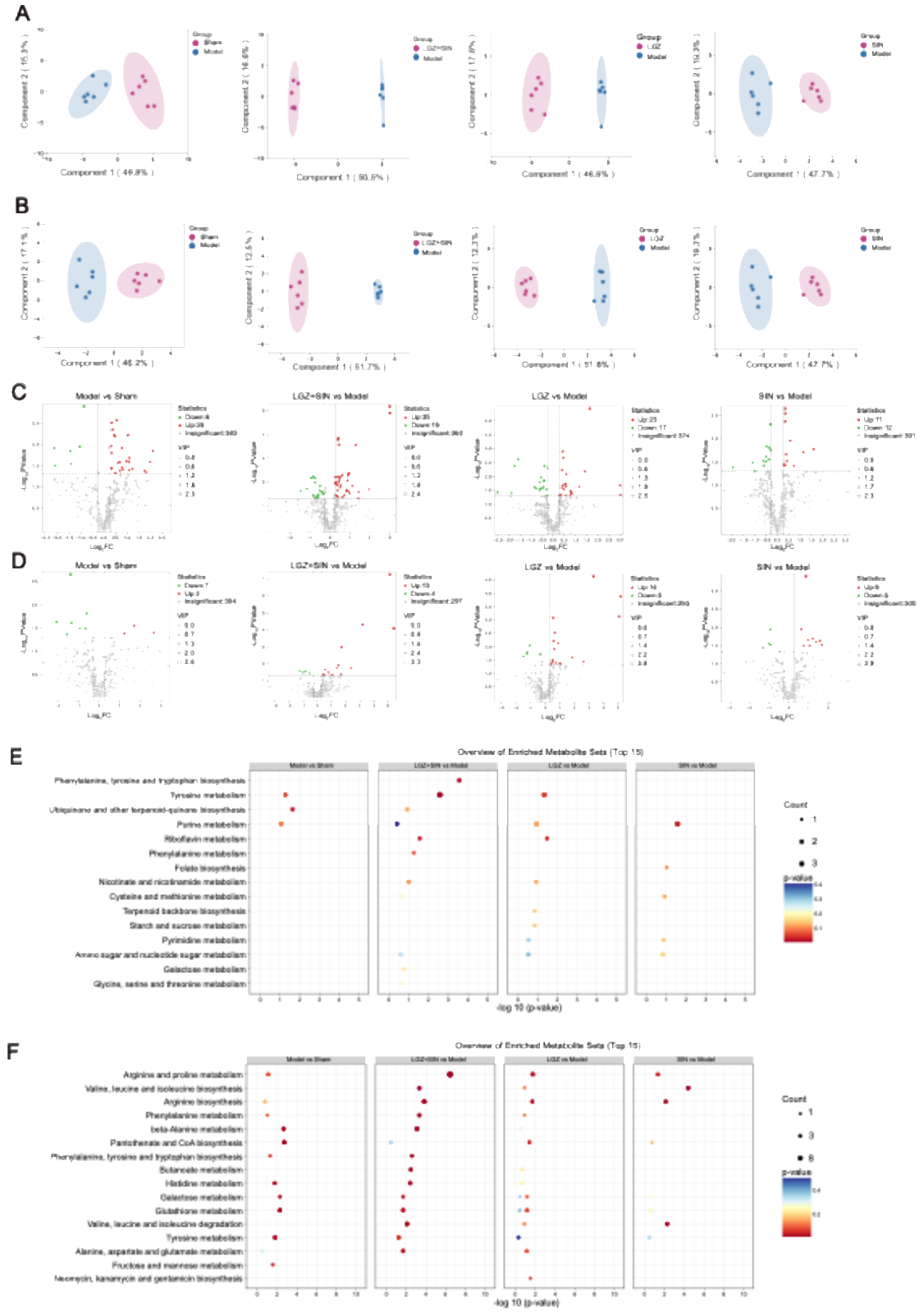

Figure 4. Metabolite changes in CCI rats following the LGZ+SIN intervention. (A) Results of OPLS-DA scores scatter plot of CSF samples. (B) Results of OPLS-DA scores scatter plot of plasma samples. (C) Volcano plot of metabolites in CSF samples. (D) Volcano plot of metabolites in plasma samples. (E). The metabolic pathways of differential metabolites in CSF samples. (F) The metabolic pathways of differential metabolites in plasma samples.

Preprints.org (www.preprints.org) | NOT PEER-REVIEWED | Posted: 23 January 2025 doi:10.20944/preprints202501.1776.v1

To further validate the results, a t-test was conducted to examine whether significant differences existed between the groups. Differential metabolites between the Sham and Model groups, as well as between treatment groups and the Model group, were identified. This approach confirmed te presence of significant metabolic changes, offering further insights into the therapeutic effects of the treatments on the CCI rats.

As shown in Figure4 C-D, metabolites that increased significantly ($p < 0.05$) with a FC >1.2 were marked red; metabolites that decreased significantly ($p < 0.05$) and exhibited a FC >1.2 were marked green.

In the plasma samples, a total of 32 differential metabolites were identified between the Model and Sham groups, with 26 metabolites were up-regulated and 6 were down-regulated. Compared to the Model group, 54 differential metabolites were identified in the LGZ+SIN group, including 35 upregulated and 19 downregulated. In the LGZ group, 40 differential metabolites were detected compared to the Model group, with 23 upregulated and 17 downregulated. In the SIN group, 23 differential metabolites were identified compared to the Model group, with 11 upregulated and 12 downregulated. From the perspective of the number of differential metabolites, the LGZ+SIN group exhibited a total of 54 differential metabolites, which is 14 more than those in the LGZ group and 31 more than those in the SIN group. In the CSF samples, 10 differential metabolites were identified between the Model and Sham groups, with 3 metabolites upregulated and 7 downregulated. In the LGZ+SIN group compared to the Model group, 17 differential metabolites were identified, with 13 upregulated and 4 downregulated. In the LGZ group compared to the Model group, 21 differential metabolites were identified, with 16 upregulated and 5 downregulated. In the SIN group, 14 differential metabolites were identified, with 9 upregulated and 5 downregulated. From the perspective of the number of differential metabolites, the LGZ+SIN group showed a greater effect on changes in the metabolic profile in CSF.

2.3.2. Metabolomic Pathway Analysis

To identify the metabolic pathways most relevant to the pain-relieving effect of the combined use of LGZ and SIN in CCI rats, Metaboanalyst 6.0 software was used to analyze the metabolic pathways. Pathways with an impact value (impact > 0) were selected as the screening criterion.

In plasma samples, the Model group primarily interfered with 28 metabolic pathways, including tyrosine metabolism, phenylalanine, tyrosine and tryptophan biosynthesis, and beta-alanine metabolism, which contribute to the development of neuropathic pain and related symptoms. The LGZ+SIN group primarily modulated 29 metabolic pathways, including arginine and proline metabolism, phenylalanine metabolism, phenylalanine, tyrosine and tryptophan biosynthesis, arginine biosynthesis, alanine, aspartate and glutamate metabolism, beta-alanine metabolism, and tyrosine metabolism. The LGZ group primarily modulated 28 pathways, including arginine biosynthesis, arginine and proline metabolism, and phenylalanine metabolism. The SIN group primarily regulated 14 pathways, including cysteine and methionine metabolism, phenylalanine, tyrosine and tryptophan biosynthesis, phenylalanine metabolism, and arginine biosynthesis. From the perspective of the number of metabolic pathways regulated, LGZ+SIN influences one more pathway than LGZ and fourteen more than SIN. Moreover, LGZ+SIN regulated several metabolic pathways that involved four or more differential metabolites, facilitating the identification of key metabolic pathways (Figure 4E).

In CSF samples, the Model group primarily modified with three pathways, including tyrosine metabolism and purine metabolism, contributing to the occurrence of neuropathic pain-related symptoms. The LGZ+SIN group primarily modulates 12 pathways, including tyrosine metabolism, riboflavin metabolism, and phenylalanine metabolism. The LGZ group regulated 11 pathways, including tyrosine metabolism, riboflavin metabolism, and tryptophan metabolism. The SIN group primarily affected 5 pathways, including purine metabolism (Figure 4F).

Based on these results and in conjunction with the KEGG database, the key metabolic pathways involved in LGZ and SIN intervention in NP include the tyrosine metabolism pathway and the phenylalanine metabolism pathway (Figure 5).

Preprints.org (www.preprints.org) | NOT PEER-REVIEWED | Posted: 23 January 2025 doi:10.20944/preprints202501.1776.v1

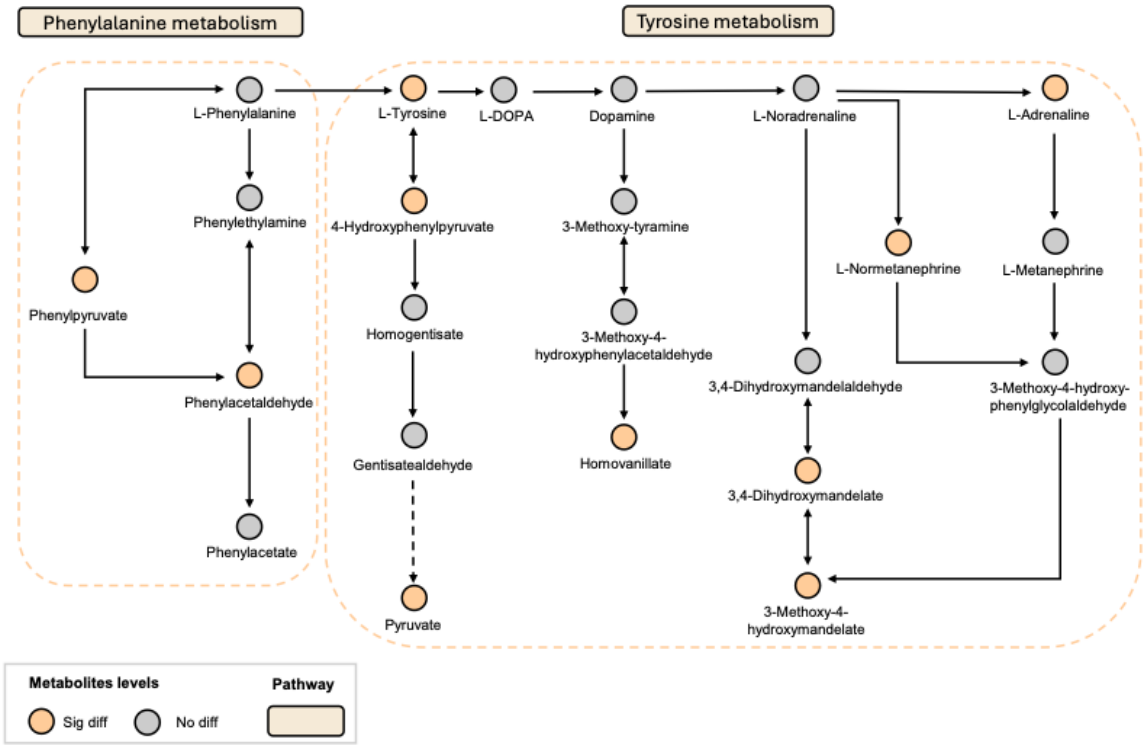

Figure 5. LGZ and SIN intervene in key metabolic pathways of CCI rats.

2.3.3. The Combination of LGZ and SIN Altered the Metabolites of Biological in CCI Rats

In the plasma samples, LGZ+SIN significantly increased the levels of 5-Hydroxytryptophan, Normetanephrine, Anserine, and Carnosine, while significantly decreasing the levels of Phenylpyruvate and N-Methylaspartate. Additionally, LGZ+SIN notably increased the levels of Epinephrine, Tryptophan, and Spermine, while decreasing the levels of 3-Methoxy-4-Hydroxymandelate and N-Acetylphenylalanine. LGZ significantly increased the levels of 5-Hydroxytryptophan and notably decreased the levels of 5-Hydroxytryptophol and 3-Methoxy-4-Hydroxymandelate. LGZ also increased the levels of Epinephrine, Normetanephrine, Tryptophan, Spermine, Anserine, and Carnosine, while decreasing the levels of Phenylpyruvate, N-Acetylphenylalanine, and N-Methylaspartate. SIN significantly increased the levels of 5-Hydroxytryptophan, Epinephrine, Tryptophan, Spermine, Anserine, and Carnosine, while notably decreasing the levels of 3-Methoxy-4-Hydroxymandelate, N-Acetylphenylalanine, and N-Methylaspartate.In the targeted analysis of neurotransmitter-related metabolites in plasma samples, LGZ+SIN significantly decreased the levels of 4-Aminobutyric acid and Serotonin, while notably improving the levels of 3-Methoxytyramine, 5-Hydroxytryptophan, Choline, Dopamine, Glutamine, Picolinic acid, and Quinolinic acid. LGZ and SIN both significantly decreased the levels of 4-Aminobutyric acid. LGZ also significantly reduced the level of Dopamine, while improving the levels of 3-Methoxytyramine, Aspartate, Choline, Glutamine, Norepinephrine, Picolinic acid, Quinolinic acid, Serine, and Serotonin. SIN notably improved the levels of 3-Methoxytyramine, Aspartate, Dopamine, Glutamate, Glutamine, Kynurenine, Norepinephrine, Phenylalanine, Quinolinic acid, and Serotonin (Figure 6A).

In the CSF samples, the combination of LGZ and SIN significantly rebalanced the levels of 3-(4-Hydroxyphenyl) Pyruvate and Normetanephrine, and notably adjusted the levels of Dopamine and L-Dopa, while reducing the level of N-methyl-L-glutamic acid. LGZ significantly reduced the level of N-methyl-L-glutamic acid, while also rebalancing 3-(4-Hydroxyphenyl) Pyruvate, and reducing 3-Nitrotyrosine, Dopamine, and L-Dopa levels. SIN significantly rebalanced Normetanephrine levels and notably adjusted the levels of L-Dopa and N-methyl-L-glutamic acid (Figure 6B).

Preprints.org (www.preprints.org) | NOT PEER-REVIEWED | Posted: 23 January 2025 doi:10.20944/preprints202501.1776.v1

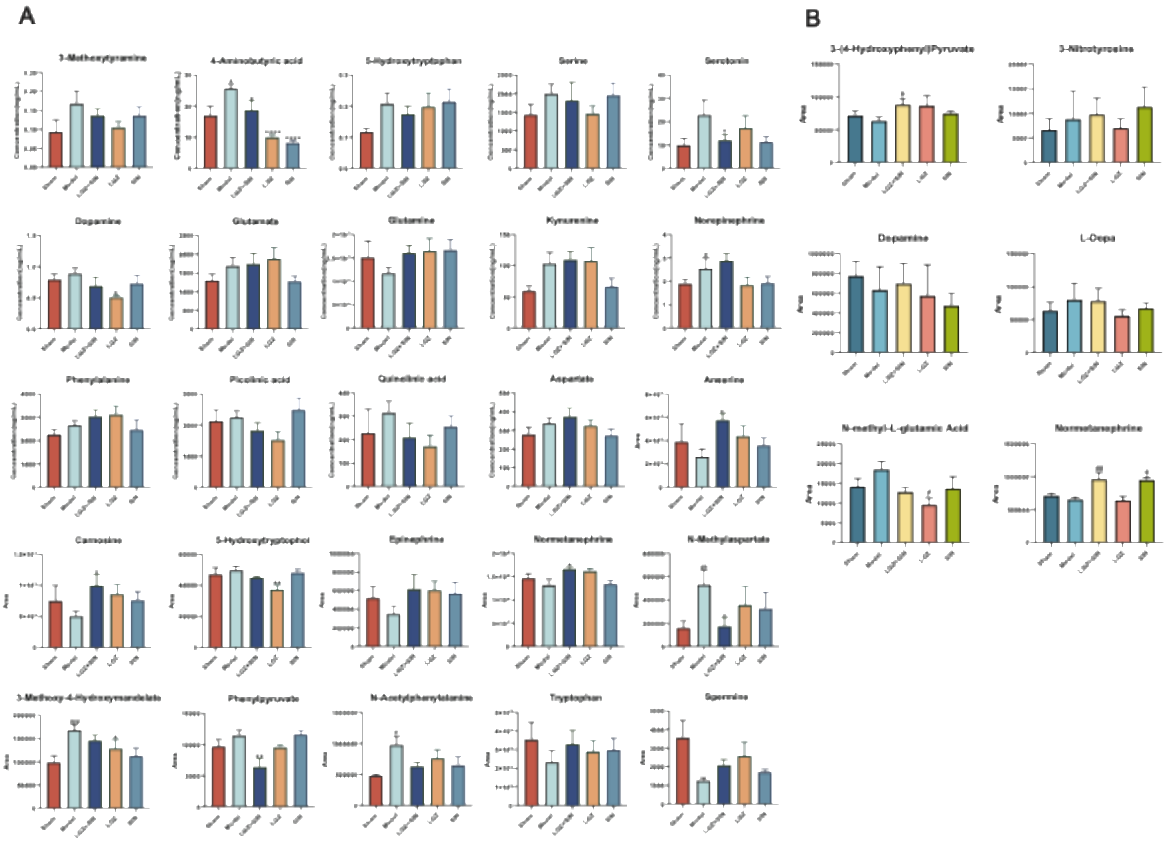

Figure 6. LGZ+SIN alters the metabolites of biological samples in CCI rats. (A) plasma. (B) CSF.

2.4. Joint Pathways Analysis

Using the "Joint-Pathway Analysis" module in Metaboanalyst 6.0, we performed an association analysis between the 34 core targets of LGZ and SIN predicted by network pharmacology and the differentially regulated metabolites in the plasma metabolomics of the combined use of LGZ and SIN (Figure 7A). The analysis identified 11 pathways with a $p < 0.05$, of which 5 pathways were enriched with both network pharmacology targets and differential metabolites from metabolomics. These pathways included arginine and proline metabolism, phenylalanine metabolism, arginine biosynthesis, histidine metabolism, and tyrosine metabolism. Further analysis of 9 core targets of LGZ with the plasma differential metabolites revealed 5 pathways with a $p < 0.05$, of which 2 pathways—phenylalanine metabolism, arginine and proline metabolism—were enriched with both targets and metabolites. For SIN, the analysis of its 25 core targets with plasma differential metabolites resulted in 8 pathways with a $p < 0.05$, with 3 pathways simultaneously enriched with network pharmacology targets and metabolomics differential metabolites. These included arginine and proline metabolism, arginine biosynthesis, and tyrosine metabolism.

Preprints.org (www.preprints.org) | NOT PEER-REVIEWED | Posted: 23 January 2025 doi:10.20944/preprints202501.1776.v1

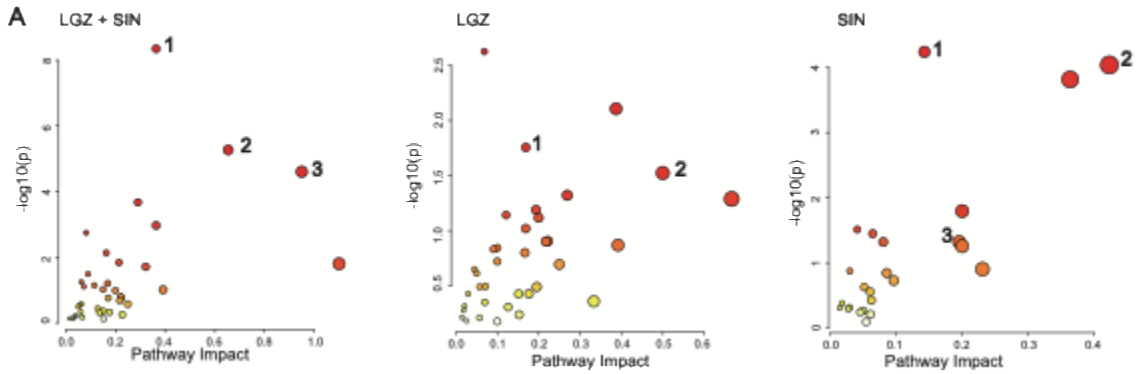

Group	Pathways name	Matched targets	Matched metabolites
LGZ+SIN	1.Arginine and proline metabolism	NOS1, NOS2, MAOA, MAOB	HMDB0000517, HMDB0000128, HMDB0001256, HMDB0001257, HMDB0001366, HMDB0000214, HMDB0003464, HMDB0000243
	2.Arginine biosynthesis	NOS1, NOS2	HMDB0000517, HMDB0000904, HMDB0000214, HMDB0000208
	3.Phenylalanine metabolism	MAOA, MAOB	HMDB0006236, HMDB0000205, HMDB0000158
	4.Histidine metabolism	MAOA, MAOB	HMDB0000033, HMDB0000194, HMDB0002024
	5.Tyrosine metabolism	MAOA, MAOB	HMDB0000208, HMDB0000118, HMDB0000243
LGZ	1.Arginine and proline metabolism	MAOA	HMDB0000064, HMDB0000162, HMDB0000214
	2. Phenylalanine metabolism	MAOA	HMDB0006236
SIN	1. Arginine and proline metabolism	NOS1, NOS2, MAOA, MAOB	HMDB0000214, HMDB0003464
	2. Arginine biosynthesis	MAOA, MAOB	HMDB0000214, HMDB0000904
	3.Tyrosine metabolism	MAOA, MAOB	HMDB0000291

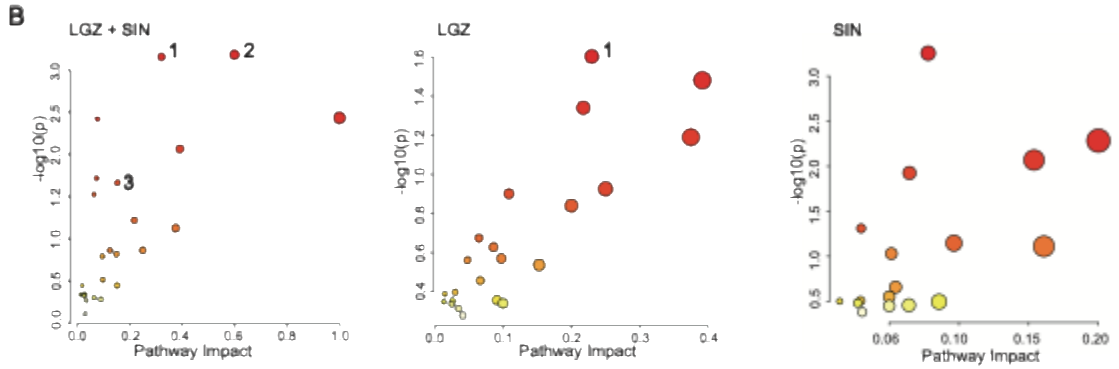

Group	Pathways name	Matched targets	Matched metabolites
LGZ+SIN	1. Tyrosine metabolism	MAOA, MAOB	HMDB0001866, HMDB0000819, HMDB0000707
	2. Phenylalanine metabolism	MAOA, MAOB	HMDB0000205
	3. Glycine, serine and threonine metabolism	MAOA, MAOB	HMDB0001721
LGZ	1. Tyrosine metabolism	MAOA	HMDB0001866, HMDB0000819
SIN	-	-	-

Figure 7. Joint pathway analysis: matched targets and metabolites. (A) Joint pathway analysis of CSF samples. (B) Joint pathway analysis of plasma samples.

The combined findings suggest that the phenylalanine metabolism, tyrosine metabolism, arginine and proline metabolism pathways could be key metabolic pathways in the pain-relieving effects of LGZ and SIN. LGZ may primarily influence tyrosine metabolism in the cerebrospinal fluid and phenylalanine metabolism in the plasma, while SIN appears to mainly regulate tyrosine metabolism in the plasma.

The analysis of the number of pathways with a $p < 0.05$, enriched by both network pharmacology and plasma metabolomics, showed that LGZ+SIN regulated 6 more pathways than ligustrazine and 3 more than SIN. Furthermore, LGZ+SIN enriched 3 more pathways with both network pharmacology targets and differential metabolites compared to LGZ and 2 more than SIN.

Association analysis of the 34 core targets of LGZ and SIN derived from network pharmacological predictions with differential metabolites regulated by LGZ+SIN in CSF

Preprints.org (www.preprints.org) | NOT PEER-REVIEWED | Posted: 23 January 2025 doi:10.20944/preprints202501.1776.v1

metabolomics (Figure 7B). The results revealed 8 pathways with a $p < 0.05$, of which 3 pathways - tyrosine metabolism, phenylalanine metabolism, and glycine, serine and threonine metabolism were significantly enriched with both network pharmacology targets and differential metabolites. These three pathways were considered the primary metabolic pathways by which LGZ+SIN regulated pain. Among these, tyrosine metabolism contained the highest number of targets and differential metabolites, making it the most critical pathway. For LGZ, the association analysis with the CSF metabolites revealed 3 pathways with a $p < 0.05$, with only one pathway (tyrosine metabolism) being enriched with both network pharmacology targets and differential metabolites. For SIN, the analysis showed 5 pathways with a $p < 0.05$, but none of these pathways were enriched with both network pharmacology targets and CSF differential metabolites.

Overall, the pathway enrichment analysis demonstrated that LGZ+SIN regulated more pathways with a $p < 0.05$ than either LGZ (by 5 pathways) or SIN (by 3 pathways). Additionally, pathways enriched with both network pharmacology targets and differential metabolites were more abundant in LGZ+SIN, with 3 pathways more than LGZ and 2 pathways more than SIN.

3. Discussion

NP is a secondary condition to various clinical disorders and significantly impacts on patients' quality of life. However, the precise pathogenesis of NP poorly understands, involving complex interactions of multiple signaling pathways and targets. Studies have demonstrated that in a spinal cord injury-induced NP rat model, tyrosine metabolism was disrupted, with dopamine levels significantly lower compared to normal rats[24]. Furthermore, the levels of phenylalanine and tyrosine in the CSF of patients with localized pain syndromes were markedly elevated[25]. Therefore, multi-drug combination therapies, encompassing both combined pharmaceutical agents and multi-target TCM, can partially address clinical treatment needs. However, for certain drugs with unclear mechanisms, it is essential to identify their key therapeutic targets. Small molecules derived from natural products or TCM frequently exhibit multi-target properities, complicating the precise identification of their therapeutic targets[26]. Thus, employing metabolomics or network analysis techniques analysis to investigate the mechanism of action of these drugs through the modulation of entire metabolic pathways or networks could represent a promising approach[27]. Chuanxiong Rhizoma and Sinomenii Caulis, widely utilized in clinical practice as TCM, have long been recognized for their substantial efficacy in treating various pain-related diseases. Based on those findings, we selected their active components, LGZ and SIN, for combined application, with the aim of exploring their potential therapeutic effects on NP.

In previous studies, we investigated the analgesic effects of the combined use of LGZ and SIN in models of inflammatory pain, sciatic nerve injury, and spinal cord injury NP [18]. Given that the CCI model simulated both neuropathic and inflammatory pain characteristics, we examined the analgesic effects of LGZ and SIN in combination, as well as individually, in the CCI model rats to comprehensively assess the advantage benefits of their combined use. In prior research, LGZ and SIN were administered via intraperitoneal injection[16], whereas both have established oral administration protocols[28,29]. Therefore, in this study, we evaluated the analgesic effects of the oral administration of LGZ and SIN in combination. Additionally, the experimental design assessed the analgesic effects of various dosages and time points for both combined and single-drug treatments to fully characterize the analgesic properties of the LGZ-SIN combination. The results from the MWT test, cold allodynia test, and incapacitance test demonstrated that the combined use of LGZ and SIN, as well as individual treatments, effectively alleviated mechanical allodynia, cold pain sensitivity, and spontaneous pain in CCI-induced NP. Furthermore, the combination of LGZ and SIN exhibited significant greater analgesic effects than single-drug treatments, reinforcing the rationale for their combined use. Moreover, the results suggested that the combined use of LGZ and SIN also produced beneficial effects on sciatic nerve inflammation and repair in CCI rats. Following the evaluation of LGZ, SIN, and their combination, we conducted network pharmacology and metabolomics studies to explore their potential mechanisms in treating NP.

The network pharmacology approach elucidated the analgesic mechanism of the combined use of LGZ and SIN starting from these two substances. First, both LGZ and SIN exhibited multi-target

Preprints.org (www.preprints.org) | NOT PEER-REVIEWED | Posted: 23 January 2025 doi:10.20944/preprints202501.1776.v1

properties. Second, pathway analysis confirmed that both LGZ and SIN could regulate multiple signaling pathways to exert their synergistic effects. Based on network pharmacology results, modulation of the tyrosine metabolism and phenylalanine metabolism pathway might be the key mechanisms through which the combined use of LGZ and SIN exerted its analgesic effects.

Given that NP affects both peripheral and central systems, this study analyzed plasma and CSF samples to investigate the metabolic regulatory effects of the combined use of LGZ and SIN, as well as their individual effects, on CCI rats. The results of metabolic pathway analysis showed that the combined treatment of LGZ and SIN regulated more metabolic pathways in both CSF and plasma samples compared to either LGZ or SIN used alone, exhibiting a synergistic effect. Finally, joint pathway analysis revealed that tyrosine metabolism and phenylalanine metabolism were the pathways enriched in both CSF and plasma samples. These pathways were considered the most critical. Among these, LGZ had a greater impact on tyrosine metabolism in CSF, while SIN exhibited a stronger effect on tyrosine metabolism in plasma. The arginine and proline metabolism pathways contained the most targets and differential metabolites enriched by the combined treatment of LGZ and SIN in plasma samples. Therefore, the combined treatment of LGZ and SIN might alleviate pain in the CCI model rats by jointly regulating tyrosine metabolism and phenylalanine metabolism in the CSF and plasma, as well as regulating arginine and proline metabolism in the plasma.

Tyrosine is an essential amino acid, and phenylalanine serves as its precursor. Both tyrosine and phenylalanine are precursors to monoamine neurotransmitters, including dopamine, norepinephrine, and epinephrine. The descending monoaminergic pathways, particularly norepinephrine and serotonin transmission, played a crucial role in the endogenous pain modulation system, a mechanism confirmed in NP[30]. Studies have shown that CCI resulted a reduction of neurotransmitters crucial to the descending pain regulation pathways, such as serotonin and norepinephrine[31]. Moreover, antidepressants that inhibited the reuptake of norepinephrine and serotonin have been shown to be effective in chronic neuropathic pain[5]. Metabolomics results showed that serotonin and its precursor, tryptophan, were reduced in the plasma of the Model group, but their levels were restored after treatment. The LGZ+SIN group demonstrated a more pronounced recovery compared to individual treatments. Arginine, a non-essential amino acid, serve as a precursor for nitric oxide, proline, and glutamate. Studies have demonstrated that arginine could increase pain sensitivity in animal models[32]. Small-scale patient studies have suggested that L-arginine might have an analgesic effect in chronic pain[33]. The central glutamatergic system played a critical role in the onset and persistence of persistent pain, including both neuropathic and inflammatory pain[34]. Following nerve injury, the downregulation of GABA and opioid receptors in the spinal cord increased glutamate release, which might contribute to the development of neuropathic pain[35]. Studies have shown that CCI-induced NP reduced GABA levels and neuronal activity in the dorsal horn[36]. Furthermore, the glutamatergic system could exacerbate chronic neuropathic pain by activating N-methyl-D-aspartate receptors (NMDARs) [37]. Some studies have suggested that inhibiting NMDARs could alleviate the severity of NP[38]. In the metabolomics analysis, the decrease in glutamine levels in the Model group and the subsequent recovered following treatment may be associated with this effect.

To the best of our knowledge, this is the first report on the therapeutic effects and potential mechanisms of combining LGZ and SIN for the treatment of neuropathic pain induced by CCI, using metabolomics and network pharmacology approaches. However, some limitations remain at the current stage. Further research is needed to elucidate the detailed mechanisms underlying the combined use of LGZ and SIN in treating CCI rats, with particularly focus on their targets and associated metabolic signaling pathways.

4. Materials and Methods

4.1. Animals and Treatment

Adult male Sprague-Dawley rats (180-200g) were obtained from Beijing Hfk Biosicence Co., Ltd. 3 rats were housed per cage in SPF-grade lab at a constantly maintained temperature (22 ± 2°C) with a 12-hour light/dark cycle and allowed free access to food and water.

Preprints.org (www.preprints.org) | NOT PEER-REVIEWED | Posted: 23 January 2025 doi:10.20944/preprints202501.1776.v1

Following the successful establishment of the model, 42 rats were randomly assigned into 7 groups, with 6 animals per group. The groups were as follows: Model group (Model, 10 ml·kg^{-1}·d saline), LGZ+SIN low-dose group(LGZ 25 mg·kg^{-1}·d+SIN 25 mg·kg^{-1}·d),LGZ+SIN medium-dose group(LGZ 50 mg·kg^{-1}·d+SIN 50 mg·kg^{-1}·d), LGZ+SIN high-dose group (LGZ 25 mg·kg^{-1}·d+SIN 25 mg·kg^{-1}·d), Ligustrazine group (LGZ, 100 mg·kg^{-1}·d^{-1}), Sinomenine group (SIN, 100 mg·kg^{-1}·d^{-1}), Pregabalin positive control group (Pgb, 30 g·kg^{-1}·d^{-1}). In addition, 6 healthy rats were set as the sham operation group (Sham, 10ml·kg^{-1} saline). All animals were orally administered their respective treatments twice daily (morning and evening) for a period of three consecutive days.

4.2. Chemicals and Materials

The Easyflow independent ventilation cage was purchased from Tecniplast, Italy. The Von Frey filaments were obtained from Ugo Basile Biological Apparatus Conpany. The pain testing frame was made in our laboratory.

The HPLC-MS/MS system (AB Sciex, USA) comprised an ExionLC-20AC high-performance liquid chromatography (HPLC) system, Ion Drive™ Turbo V ion source, Sciex 6500^{+} triple quadrupole mass spectrometer, Analyst 1.7 data acquisition software, and MultiQuant 3.0.3 data processing software. The Targin VX-Ⅲ multi-tube vortexer was purchased from Beijing Tajin Technology Co., Ltd. The Forma 88000 Series −86°C ultra-low temperature freezer was obtained from Thermo Scientific (USA). The Rotanta 460R high-speed refrigerated centrifuge was acquired from Hettich (Germany). The MC-8 integrated cryogenic centrifuge concentrator was obtained from Beijing Jiaime Technology Co., Ltd. The Synergy2 multifunctional microplate reader was purchased from BioTek (USA). The desktop anesthetic machine was supplied by Harvard Apparatus (USA). The ThermoStar body temperature maintenance device was purchased from RWD Life Science Co., Ltd. The optical microscope (Olympus BX50) was purchased from Olympus Optical Co. (Tokyo, Japan).

Ligustrazine (Ligustrazine Hydrochloride, lot number: DT201803-19) and Sinomenine (Sinomenine Hydrochloride, lot number: DT201806-22), both with a purity ≥98% were provided by Shanxi Datian Biotechnology Ltd. (Xian, China). Pregabalin (lot number: 295422) was provided by Beijing Jiaime Technology Co., Ltd. The isoflurane (lot number: 217180801) was purchased from RWD Life Science Co., Ltd.

IL-6, IL-1β, and TNF-α ELISA kits were purchased from Raybiotech. The tissue lysis buffer (EL-lysis) was obtained from Raybiotech. The BCA protein assay kit was purchased from Thermo Fisher. The 4-0 chromic gut sutures were obtained from Shandong Boda Medical Products Co., Ltd.

Mass spectrometry library kits and reference standards for glucose metabolism, amino acids, bile acids, and others were purchased from Sigma for the establishment of a widely targeted metabolomics analysis platform in our laboratory. Internal standards, including d-3 norepinephrine, d-4 dopamine-D4, d-5 serotonin, and MSK-A2, were obtained from Cambridge Isotope Laboratories. Reference standards for metabolic pathways, including tyrosine, sodium borate, benzoyl chloride, and d-5 benzoyl chloride were purchased from Sigma. All reference and internal standards had a purity greater than 99%. LC/MS-grade acetonitrile, methanol, formic acid, and ammonium formate were obtained from Beijing Dikema Technology Co., Ltd.

4.3. CCI Model Establishment

The CCI model in rats was established following the method described by Bennett [21]. After anesthetizing the rats with isoflurane, they were placed on a heating pad to maintain a body temperature of approximately 37°C. The skin below the left femur was incised and the left sciatic nerve was exposed after blunt separation from the surrounding tissue. The nerve was then ligated with 4–0 chromic gut suture at four knots, each approximately 1 mm apart. The degree of ligation was adjusted to induce slight twitching of the calf muscles without compromising the blood supply to the nerve epineurium. In the sham group, the sciatic nerve was exposed but left unligated. The mechanical withdrawal threshold (MWT) test was conducted both prior to surgery and on day 7 post-surgery to assess the success of the model.

4.4. Pharmacodynamic Research

Preprints.org (www.preprints.org) | NOT PEER-REVIEWED | Posted: 23 January 2025 doi:10.20944/preprints202501.1776.v1

The body weight of the rats was recorded daily. Behavioral tests were conducted on days 1, 2, and 3 following drug administration. The behavioral tests included the MWT test, cold allodynia test, and incapacitance test. The MWT and cold allodynia test were conducted at 0, 0.5, 2, 4, and 6 hours following drug administration each day. The incapacitance test was conducted 4 hours following drug administration each day. After the final behavioral test, samples of the affected sciatic nerve were collected for hematoxylin and eosin (HE) staining and enzyme-linked immunosorbent assay (ELISA) analysis. Plasma and CSF samples were also collected for subsequent metabolomic analysis.

The MWT test was assessed using Von Frey filaments[39]. The rats were placed in a plastic chamber (20 cm×20 cm×15 cm) with a transparent acrylic lid and allowed to habituate for 30 minutes. Von Frey filaments ranging from 4 g to 26 g were used during the test. The "up-and-down" method was employed to determine the MWT value of each rat[40].

The cold allodynia test was performed by spraying 0.1 mL of acetone on the affected hind paw of the rat. The responses of the rats, including paw withdrawal and licking behavior, were observed, and scored based on the degree of reaction: 0 points for no response; 1 point for mild reaction or rapid withdrawal of the hind paw; 2 points for repeated paw shaking; 3 points for sustained or repeated lifting and licking of the hind paw[41].

The incapacitance test was conducted by placing the rats in a transparent box equipped with an inclined platform, where the rats stood on their hind feet. The left and right hind feet were position on separate sensor panels. Care was taken to ensure that the rats maintained an exploratory posture, without leaning against the sides of the box. A capacimeter was used to measure the weight (in grams) on each panel over a 3-second period. Each rat underwent three measurements, with a minimum of 1 minute between each reading. The average of the readings for each hind foot was used to calculate the weight distribution. The bipedal balance bearing value was recorded as the percentage of total body weight supported by each hind foot. In normal rats, weight distribution is nearly symmetrical (50:50%), whereas pain resulting from injury leads to a reduction in the load-bearing capacity of the injured hind foot. The bipedal balance b average earing result was calculated using the following formula: Result = Weight on the affected hind foot / (Weight on the left hind foot+ Weight on the right hind foot) ×100%[42].

The sciatic nerve tissue was fixed in 4% paraformaldehyde and subsequently embedded in paraffin to prepare 5 μm thick sections. The sections were stained with hematoxylin for 5 minutes, followed by eosin staining for 3 minutes. Changes in the sciatic nerve were observed using an optical microscope.

The concentrations of IL-1β, IL-6, and TNF-α in the sciatic nerve were measured using ELISA. The experimental procedure was strictly adhered to, following the instructions provided with the kits. The final concentrations were corrected using the total protein content of the sciatic nerve.

4.5. Network Pharmacology Analysis

First, the potential targets of LGZ and SIN were identified using the SWISS Target Prediction database (http://swisstargetprediction.ch/). These targets were then verified and refined using the UniProt database to obtain accurate target names for each compound. Subsequently, pain-related target information was obtained from the Genecards database (https://www.genecards.org/) and the OMIM database (https://omim.org/). After removing duplicates, the remaining targets were regarded as pain-related targets for further analysis. The intersection of LGZ and SIN alkaloid targets with those associated with pain was identified using the Bioinformatics platform (http://www.bioinformatics.com.cn), yielding common genes across the different compounds. This gene set was then analyzed based on the distinctiveness of the drug-target interactions.

Next, the intersecting target genes were inputted into the STRING database to construct a Protein-Protein Interaction (PPI) network. The network was visualized using Cytoscape 3.8.2, and the CytoHubba plugin was employed to identify the core targets for further differential analysis.

Finally, the core target genes underwent Gene Ontology (GO) and Kyoto Encyclopedia of Genes and Genomes (KEGG) enrichment analysis using the Metascape database. A significance threshold of $P < 0.01$ was set for all analyses. The GO analysis encompassed three subcategories: Biological Process (BP), Molecular Function (MF), and Cellular Component (CC). Furthermore, based on the

Preprints.org (www.preprints.org) | NOT PEER-REVIEWED | Posted: 23 January 2025 doi:10.20944/preprints202501.1776.v1

relationships between protein targets and signaling pathways, a compound-target-pathway association network was constructed.

4.6. Plasma and CSF METABOLOMICS ANALYSIS

4.6.1. Plasma and CSF SAMPLE PREPARATION

For the sample preparation, 50 μL of the test sample was combined with 450 μL of ice-cold extraction solvent containing internal standards (methanol: acetonitrile: water = 2:2:1). The mixture was vortexed for 3 minutes, then placed at -20°C for 2 hours. Subsequently, the samples were centrifuged at 20,000 g for 15 minutes at 4°C. The supernatant was carefully transferred to a 1.5 mL Eppendorf tube and subjected to vacuum concentration at 35°C and 1,500 rpm for 2 hours. The residue was reconstituted with 100 μL of extraction solvent devoid of internal standards. The sample was centrifuged again at 20,000 g for 15 minutes at 4°C, and 80 μL of the supernatant was collected for analysis. Additionally, 10 μL of each sample was pipetted to pool a quality control (QC) sample.

4.6.2. Widely Targeted Metabolomics Analysis

Metabolites were identified using a self-established reference database. An ACQUITY UPLC BEH Amide column (2.1×50 mm, 1.7 μm, Waters, USA) and a pre-column (2.1 mm×5 mm, 1.7 μm, Waters) were used to separate samples. The mobile phase consisted of solvent A (95% water: 5% acetonitrile, containing 5 mM ammonium formate and 0.01% formic acid) and solvent B (95% acetonitrile: 5% water, containing 5 mM ammonium formate and 0.01% formic acid). The gradient elution program was as follows: 0-2 min, 95-95% B; 2-4 min, 95-90% B; 4-6 min, 90-90% B; 6-9 min, 90-85% B; 9-12 min, 85-85% B; 12-15 min, 85-75% B; 15-16 min, 75-75% B; 16-18 min, 75-50% B; 18-20 min, 50-50% B; 20-22 min, 50-25% B; 22-24 min, 25-25% B; 24-25 min, 25-95% B; 25-30 min, 95-95% B. Flow rate: 0.3 mL/min; column temperature: 35°C; temperature: 4°C; injection volume: 5 μL.

Electrospray ionization (ESI) was used as the ionization source. The curtain gas (N_2) was set to 40 psi, collision gas (N_2) to 9 psi, and the spray voltage was set at +5500 V and -4500 V for positive and negative ion modes, respectively. The nebulizer temperature was set to 550°C, with ion source gas (Ion Source Gas1, N_2) and auxiliary gas (Ion Source Gas2, N_2) both set to 55 psi. Scanning was performed in both positive and negative ion modes. Optimized ion pairs and mass spectrometry parameters were applied for each metabolite.

4.6.3. Targeted Metabolomics Analysis

The method for measuring the tyrosine pathway was adapted from previously published protocols[43] with necessary modifications outlined below.

Sample preparation: A 50 μL aliquot of the sample was mixed with 150 μL of acetonitrile (1:3, v/v). The mixture was vortexed at 8,000 rpm for 5 minutes, followed by centrifugation at 20,000 g for 10 minutes. Subsequently, 10 μL of the supernatant was transferred and added to 10 μL of 100 mM sodium borate and 10 μL of 1% benzoyl chloride. The mixture was vortexed for 5 minutes, incubated at 25°C for 5 minutes, and then centrifuged at 20,000 g for 10 minutes. The resulting supernatant (24 μL) was mixed with 6 μL of an internal standard solution (a mixture of tyrosine pathway standards and d-5 benzoyl chloride for derivatization). The mixture was then vortexed and prepared for injection.

A PFP C18 column (2.1×50 mm, 1.8 μm, Waters, USA) was used to separate samples. Water with 0.1% formic acid and 5 mM ammonium formate served as mobile phase A and acetonitrile served as mobile phase B. The gradient programs were as follows: 0-1min, 20-20% B; 1-2min, 20-50% B; 2-6min, 50-80% B; 6-6.5min, 80-95% B; 8-8.1min, 95-20% B; 8.1-10min, 20-20% B. Flow rate: 0.3 mL/min; column temperature: 35°C; sample temperature: 4°C; injection volume: 2 μL.

Electrospray ionization (ESI) was used as the ionization source. The curtain gas (N_2) was set to 35 psi, collision gas (N_2) to 9 psi, and the spray voltage was set at 5500. The nebulizer temperature was set to 550°C, with ion source gas (Ion Source Gas1, N_2) and auxiliary gas (Ion Source Gas2, N_2) both at 55 psi. The analysis was performed in Multiple Reaction Monitoring (MRM) mode with positive ion scanning. The specific ion pair parameters used for the analysis are provided in Supplementary Table S1.

Preprints.org (www.preprints.org) | NOT PEER-REVIEWED | Posted: 23 January 2025 doi:10.20944/preprints202501.1776.v1

4.6.4. Metabolomics Analysis

To ensure QC for the metabolomics analysis, a QC sample was injected after every ten experimental samples during the chromatography run. All LC-MS data underwent meticulous preprocessing using MultiQuant 3.0.3 software, including key steps such as peak detection, peak identification, peak area calculation, and calibration.

Principal component analysis (PCA) was first performed to reveal the major variability patterns within the datasets. Orthogonal partial least squares discriminant analysis (OPLS-DA) was then applied to identify differentiate metabolites that might differentiate between groups. The quality of the OPLS-DA model was evaluated using the parameters R^2Y and Q^2. Additionally, permutation testing was conducted to assess the risk of false positives in the OPLS-DA model. Potential biomarkers with significant statistical and biological relevance were selected based on the criteria: VIP > 1, t-test (p) < 0.05, and fold change (FC) > 1.2 or < 0.83. Finally, metabolic pathways associated with the differentially expressed metabolites were determined using a significance threshold of p < 0.05. The Metware Metabolomics Cloud Platform (https://cloud.metware.cn/) and Metaboanalyst 6.0 (https://www.metaboanalyst.ca/) were utilized to analyze the metabolomics data.

4.7. Joint Pathway Analysis

A joint pathway analysis was performed using the "Joint-Pathway Analysis" module in MetaboAnalyst 6.0 to correlate the key targets predicted by network pharmacology with the differential metabolites identified in the metabolomics analysis. Pathways that exhibited the highest enrichment of both targets and metabolites were considered as the key pathways.

4.8. Statistical Analysis

Data were statistically analyzed using SPSS 20.0 and GraphPad Prism 8.0. All data were shown as mean ± standard error of the mean (SEM). The significance analysis of differences between two groups was assessed using a t-test, while multiple comparison was conducted using one-way or two-way analysis of variance (ANOVA). $p < 0.05$ indicated statistical significance, and $p < 0.01$ indicated highly statistical significance.

Supplementary Materials: The following supporting information can be downloaded at: www.mdpi.com/xxx/s1.

Author Contributions: Conceptualization, Tao Li, Zhiguo Wang, Zhaoyue Yuan; methodology, Tao Li, Zhaoyue Yuan, Xiaoliang Zhao, Jidan Zhang, Yanyan Ma; software, Zhaoyue Yuan; validation, Xiaoliang Zhao; formal analysis, Xiaoliang Zhao, Yue Jiao and Yang Liu; writing—original draft preparation, Zhaoyue Yuan and Yan Zhang; investigation, Yan Zhang; resources, Chang Gao; data curation, Zhaoyue Yuan; supervision, Chang Gao, Zhiguo Wang; writing—review and editing, Tao Li, Zhaoyue Yuan and Yan Zhang. All authors have read and agreed to the published version of the manuscript.

Funding: This research was supported by the Fundamental Research Funds for the Central Public Welfare Research Institutes of China, grant number JJPY2022003, JJPY2022025, JBGS2023004, ZZ14-YQ-041 and ZZ2019004; the Scientific and Technological Innovation Project of China Academy of Chinese Medical Sciences, grant number CI2021B015; the National Natural Science Foundation of China, grant number 81503278 and T2341017.

Institutional Review Board Statement: The animal study protocol was approved by the Institutional Animal Care and Use Committee at Experimental Research Center, China Academy of Chinese Medical Sciences (No. ERCCACMS21-2111-01).

Conflicts of Interest: The authors declare no conflict of interest.

References

1. FINNERUP N B, KUNER R, JENSEN T S. Neuropathic Pain: From Mechanisms to Treatment[J]. Physiological Reviews, 2021, 101(1): 259-301.

Preprints.org (www.preprints.org) | NOT PEER-REVIEWED | Posted: 23 January 2025 doi:10.20944/preprints202501.1776.v1

2. ALLES S R A, SMITH P A. Etiology and Pharmacology of Neuropathic Pain[J]. Pharmacological Reviews, 2018, 70(2): 315-347.
3. ORHURHU M S, CHU R, CLAUS L, et al. Neuropathic Pain and Sickle Cell Disease: a Review of Pharmacologic Management[J]. Current Pain and Headache Reports, 2020, 24(9): 52.
4. HE Y, WANG Z J. Spinal and afferent PKC signaling mechanisms that mediate chronic pain in sickle cell disease[J]. Neuroscience Letters, 2019, 706: 56-60.
5. BARON R, BINDER A, WASNER G. Neuropathic pain: diagnosis, pathophysiological mechanisms, and treatment[J]. The Lancet Neurology, 2010, 9(8): 807-819.
6. JIANG B C, LIU T, GAO Y J. Chemokines in chronic pain: cellular and molecular mechanisms and therapeutic potential[J]. Pharmacology & Therapeutics, 2020, 212: 107581.
7. YOSHIMOTO Y, OKAI H, NAMBA H, et al. Combined antiallodynic effects of Neurotropin®–tramadol and Neurotropin®–mirogabalin in rats with L5-spinal nerve ligation[J]. Journal of Pharmacological Sciences, 2024, 156(1): 30-37.
8. HUNG Y C, KUTHATI Y, ZHANG X, et al. Analgesic Alkaloids Derived From Traditional Chinese Medicine in Pain Management[J]. Frontiers in Pharmacology, 2022, 13.
9. SHAO H, HE X, ZHANG L, et al. Efficacy of Ligustrazine Injection as Adjunctive Therapy in Treating Acute Cerebral Infarction: A Systematic Review and Meta-Analysis[J]. Frontiers in Pharmacology, 2021, 12: 761722.
10. MA Z, ZHANG H, ZHAO F, et al. Safety and effectiveness of Salvia miltiorrhiza and ligustrazine injection for acute cerebral infarction in Chinese population: a PRISMA-compliant meta-analysis[J]. Frontiers in Pharmacology, 2024, 15: 1425053.
11. XING Z, CHEN Y, CHEN J, et al. Metabolomics integrated with mass spectrometry imaging reveals novel action of tetramethylpyrazine in migraine[J]. Food Chemistry, 2024, 460: 140614.
12. RAO Y. Tetramethylpyrazine and Astragaloside IV have synergistic effects against spinal cord injury-induced neuropathic pain via the OIP5-AS1/miR-34a/Sirt1/NF-κB axis[J]. International Immunopharmacology, 2023.
13. HUANG Z, MAO X, CHEN J, et al. Sinomenine hydrochloride injection for knee osteoarthritis: A protocol for systematic review and meta-analysis[J]. Medicine, 2022, 101(2): e28503.
14. LI J M, YAO Y D, LUO J F, et al. Pharmacological mechanisms of sinomenine in anti-inflammatory immunity and osteoprotection in rheumatoid arthritis: A systematic review[J]. Phytomedicine, 2023, 121: 155114.
15. GAO T, HAO J, WIESENFELD-HALLIN Z, et al. Analgesic effect of sinomenine in rodents after inflammation and nerve injury[J]. European Journal of Pharmacology, 2013, 721(1-3): 5-11.
16. GAO T, LI T, JIANG W, et al. Antinociceptive Effects of Sinomenine Combined With Ligustrazine or Paracetamol in Animal Models of Incisional and Inflammatory Pain[J]. Frontiers in Physiology, 2021, 11: 523769.
17. CHEN J, GUO P, LIU X, et al. Sinomenine alleviates diabetic peripheral neuropathic pain through inhibition of the inositol-requiring enzyme 1 alpha–X-box binding protein 1 pathway by downregulating prostaglandin-endoperoxide synthase 2[J]. Journal of Diabetes Investigation, 2023, 14(3): 364-375.
18. GAO T, SHI T, WIESENFELD-HALLIN Z, et al. Sinomenine facilitates the efficacy of gabapentin or ligustrazine hydrochloride in animal models of neuropathic pain[J]. European Journal of Pharmacology, 2019, 854: 101-108.
19. MENG X. Jowiseungki decoction affects diabetic nephropathy in mice through renal injury inhibition as evidenced by network pharmacology and gut microbiota analyses[J]. 2020.
20. HU S, ZUO H, QI J, et al. Analysis of Effect of Schisandra in the Treatment of Myocardial Infarction Based on Three-Mode Gene Ontology Network[J]. Frontiers in Pharmacology, 2019, 10: 232.
21. ZHANG P, ZHANG D, ZHOU W, et al. Network pharmacology: towards the artificial intelligence-based precision traditional Chinese medicine[J]. Briefings in Bioinformatics, 2023, 25(1): bbad518.
22. YAN X Y, XIANG P, YU Z G, et al. Application of Metabonomics in Substance Abuse Toxicology Research[J]. Fa Yi Xue Za Zhi, 2022, 38(3): 400-407.

Preprints.org (www.preprints.org) | NOT PEER-REVIEWED | Posted: 23 January 2025 doi:10.20944/preprints202501.1776.v1

23. LEI C, CHEN Z, FAN L, et al. Integrating Metabolomics and Network Analysis for Exploring the Mechanism Underlying the Antidepressant Activity of Paeoniflorin in Rats With CUMS-Induced Depression[J]. Frontiers in Pharmacology, 2022, 13: 904190.
24. RODGERS H M, PATTON R, YOW J, et al. Morphine Resistance in Spinal Cord Injury-Related Neuropathic Pain in Rats is Associated With Alterations in Dopamine and Dopamine-Related Metabolomics[J]. The Journal of Pain, 2022, 23(5): 772-783.
25. MEISSNER A, VAN DER PLAS A A, VAN DASSELAAR N T, et al. 1H-NMR metabolic profiling of cerebrospinal fluid in patients with complex regional pain syndrome–related dystonia[J]. Pain, 2014, 155(1): 190-196.
26. GAN X, SHU Z, WANG X, et al. Network medicine framework reveals generic herb-symptom effectiveness of traditional Chinese medicine[J]. Science Advances, 2023, 9(43): eadh0215.
27. YAN P, WEI Y, WANG M, et al. Network pharmacology combined with metabolomics and lipidomics to reveal the hypolipidemic mechanism of Alismatis rhizoma in hyperlipidemic mice[J]. Food & Function, 2022, 13(8): 4714-4733.
28. ZHANG S, ZHENG Y, DU H, et al. The Pathophysiological Changes and Clinical Effects of Tetramethylpyrazine in ICR Mice with Fluoride-Induced Hepatopathy[J]. Molecules, 2023, 28(12): 4849.
29. GAO T, SHI T, WANG D Q, et al. Repeated sinomenine administration alleviates chronic neuropathic pain-like behaviours in rodents without producing tolerance[J]. Scandinavian Journal of Pain, 2014, 5(4): 249-255.
30. ZHAO X, WANG C, ZHANG J F, et al. Chronic curcumin treatment normalizes depression-like behaviors in mice with mononeuropathy: involvement of supraspinal serotonergic system and GABAA receptor[J]. Psychopharmacology, 2014, 231(10): 2171-2187.
31. CHAPLAN S R, BACH F W, POGREL J W, et al. Quantitative assessment of tactile allodynia in the rat paw[J]. Journal of Neuroscience Methods, 1994, 53(1): 55-63.
32. SEVERYANOVA L A, BOBYNTSEV I I, KIR'YANOVA N A, et al. Effects of L-arginine on various types of pain sensitivity[J]. Bulletin of Experimental Biology and Medicine, 2006, 141(5): 567-570.
33. HARIMA A, SHIMIZU H, TAKAGI H. Analgesic effect of L-arginine in patients with persistent pain[J]. European Neuropsychopharmacology, 1991, 1(4): 529-533.
34. OSAKA H, MUKHERJEE P, AISEN P S, et al. Complement-derived anaphylatoxin C5a protects against glutamate-mediated neurotoxicity[J]. Journal of Cellular Biochemistry, 1999, 73(3): 303-311.
35. KOHNO T, JI R R, ITO N, et al. Peripheral axonal injury results in reduced μ opioid receptor pre- and post-synaptic action in the spinal cord☆[J]. Pain, 2005, 117(1): 77-87.
36. MOON H C, PARK Y S. Reduced GABAergic neuronal activity in zona incerta causes neuropathic pain in a rat sciatic nerve chronic constriction injury model[J]. Journal of Pain Research, 2017, Volume 10: 1125-1134.
37. MEDEIROS P, NEGRINI-FERRARI S E, PALAZZO E, et al. N-methyl-d-aspartate Receptors in the Prelimbic Cortex are Critical for the Maintenance of Neuropathic Pain[J]. Neurochemical Research, 2019, 44(9): 2068-2080.
38. KIEFER R T, ROHR P, PLOPPA A, et al. Efficacy of Ketamine in Anesthetic Dosage for the Treatment of Refractory Complex Regional Pain Syndrome: An Open-Label Phase II Study[J]. Pain Medicine, 2008, 9(8): 1173-1201.
39. SHEN Y, DING Z, MA S, et al. SETD7 mediates spinal microgliosis and neuropathic pain in a rat model of peripheral nerve injury[J]. Brain, Behavior, and Immunity, 2019, 82: 382-395.
40. DEUIS J R, DVORAKOVA L S, VETTER I. Methods Used to Evaluate Pain Behaviors in Rodents[J]. Frontiers in Molecular Neuroscience, 2017, 10: 284.
41. CHEN J, JOSHI S K, DIDOMENICO S, et al. Selective blockade of TRPA1 channel attenuates pathological pain without altering noxious cold sensation or body temperature regulation[J]. Pain, 2011, 152(5): 1165-1172.
42. BUYS M J, ALPHONSO C. Novel Use of Perineural Pregabalin Infusion for Analgesia in a Rat Neuropathic Pain Model[J]. Anesthesia & Analgesia, 2014, 119(2): 481-488.

Preprints.org (www.preprints.org) | NOT PEER-REVIEWED | Posted: 23 January 2025 doi:10.20944/preprints202501.1776.v1

43. WONG J M T, MALEC P A, MABROUK O S, et al. Benzoyl chloride derivatization with liquid chromatography–mass spectrometry for targeted metabolomics of neurochemicals in biological samples[J]. Journal of Chromatography A, 2016, 1446: 78-90.

Disclaimer/Publisher's Note: The statements, opinions and data contained in all publications are solely those of the individual author(s) and contributor(s) and not of MDPI and/or the editor(s). MDPI and/or the editor(s) disclaim responsibility for any injury to people or property resulting from any ideas, methods, instructions or products referred to in the content.